Mode-selective Absorption for Spectrum Shaping

De He and Zhijun Liu*
School of Optoelectronic Science and Engineering,
University of Electronic Science and Technology of China, Chengdu, China.
vivienhede@126.com, *liuzhijun@uestc.edu.cn

Abstract. We report on realization of a spectrum shaping approach using mechanism of mode-selective absorption in a thin-film layered structure. Ultra-thin lossy films are inserted in the asymmetrical dielectric cavity at the location of nodes or antinodes of standing wave mode to reserve or absorb the energy of certain wavelengths. This layer structure can be physically regarded as the limit case of photonic crystal with limited width of forbidden band. The wavelength range and width of forbidden band can be precisely designed by tuning the thickness of each layer. The reflection spectrum is shaped into a broad rectangular flat-bottom feature by placing the ultra-thin absorber at the antinode of standing wave mode of dielectric layer. This is demonstrated experimentally via a fabricated sample. Reflection peak is also discussed theoretically by placing the absorbers at the nodes instead of antinodes to shape the reflection spectrum into a narrow peak in the desired wavelength range. The principle of this spectral shaping method is universal for the entire electromagnetic waves. It is applicable on the other fields such as the physical coloration, broadband absorption devices of energy harvest and infrared detector.

Keywords: Spectrum shaping, asymmetric dielectric cavity, mode-selective absorption.

1. Introduction

In the application of electromagnetic waves, the demand of spectral shaping has been developing to meet the ever-changing needs. In the field of communications, spectral nulls are purposefully introduced to limit interference with narrowband signals by means of shaping ultra-wideband spectrum [1]. In the radar system, spectral shaping is also employed to produce chirped microwave pulses which usually increase the time-bandwidth product, leading to an increased radar range resolution and detection distance [2]. In the visible light range, because the perceivable colors of human eyes are determined by the spectrum, the direct application of spectral shaping is the realization of man-made colors [3-5]. The plasmonic resonance mode of the optical antenna is another concerned method to realize the spectrum shaping [6-10]. The spectrum can be shaped by tuning the geometric sizes of the top plasmonic antennas to shift the resonance peak. The drawbacks of plasmonic antenna are narrow response peaks and complicated fabrication procedure. Especially in the short wavelength range, the subwavelength size of antenna calls for the costly electron beam etching which greatly limits the application in the scalable manufacturing [11-13]. Fortunately, the fabrication of layer structure is very simple and totally compatible with the existing industrial production condition. In a dielectric-metal layered structure, when the round-trip phase difference accumulated in the dielectric layer satisfies the integral/odd multiples of the wavelength/half wavelength, reflection peaks/valleys emerge due to the constructive/destructive interference. The constructive interference corresponds to a node at the top of dielectric layer. On the contrary, the destructive interference means an antinode at this interface. Since the strongest electric field is at the antinodes, in the case of destructive interference, the energy nearby the antinodes can be absorbed remarkably by a lossy layer. The famous Salisbury screen operates on this principle, in which the top glossy screen is located at the quarter of operating wavelength. It exactly corresponds to the antinode of the standing wave inside the dielectric layer, so the energy at this certain wavelength can be absorbed significantly [14]. The selective absorption ability of dielectric optical cavity allows it to be suitable for spectrum shaping by simply changing the thickness of the dielectric layer to shift the

position of reflection peak into the desired wavelength range [15-17]. On the other hand, Mikhail A. Kats et al proved that on the certain condition, replacing the dielectric layer with an ultra-thin absorbing film on a metallic substrate doesn't destroy the film interference remarkably as it was supposed to. Correspondingly, significant absorption is realized in this lossy layer, which opened the door to absorb the electromagnetic waves within ultra-thin thickness [18]. Here we proposed a multi-layer structure with ultra-thin high lossy layers on the top or inside of the dielectric cavity. It functions similarly as a photonic crystal with only few periods to precisely tailor the spectrum into the arbitrary shape. Our approach of mode-selective absorption adds an additional degree of freedom to spectrum shaping beyond that of the interferences in thin-film cavities, and is applicable to other spectral bands (e.g., IR and THz)

2. Theoretical Design

We consider a conventional asymmetric dielectric cavity formed by a SU-8 photoresist film with a thickness of 268 nm atop an Al substrate, as sketched in Fig. 1(a). In order to engineer its absorption for obtaining a target spectrum shaping, we first calculated the optical field inside the cavity via Transfer Matrix Method (TMM). The refractive indices of Al are taken from Ref. [19], and those of Ge and SU-8 were obtained from our variable angle spectroscopic ellipsometry (VASE) measurements. Our measured refractive indices of the Ge and SU-8 are close to the ones reported in Refs. 20 and 21. The solid curve in Fig. 1(b) shows the square of the absolute value of electric field inside the cavity at the wavelength of λ = 454 nm. We can see that standing wave is formed with alternating antinodes (where the electric field is the strongest) and nodes (where the electrical field is zero).

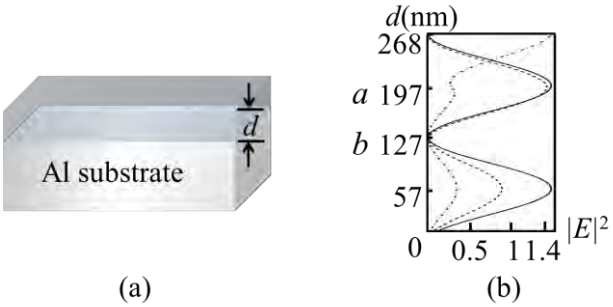

Fig .1 (a) Schematic of a dielectric cavity. (b) the square of the absolute value of electric field at the wavelength of 454 nm in dielectric layer with the cavity thickness of 268nm. The solid curve indicates the situation of none of lossy layer on or inside the dielectric cavity; the dotted curve indicates the situation of lossy layer at the antinode of 197 nm (marked as *"a"*) and the dashed curve indicates the situation of the lossy layer at the node of 127 nm (marked as *"b"*).

With information on the antinodes and nodes of electric field distribution, one can engineer the reflection spectrum of the dielectric cavity by placing absorbing materials at antinodes of undesired wavelength, while leaving other wavelengths minimally affected. Similar mode-selective absorption mechanism has been used in prior demonstrations of optical modulators and two-band infrared absorbers [22, 23]. For the SU-8 cavity described above, its simulated reflection spectrum is shown as solid curve in Fig. 2. The reflectivity is high above 80% without much wavelength selectivity on the absorption. Two reflection dips at λ = 370 nm and λ = 597 nm represent weak absorptions of the two dielectric cavity resonant modes. In order to obtain a target flat-bottom broadband reflection spectrum in such a cavity, we introduce a 14 nm lossy Ge film at the antinode of 197 nm which is labeled as *"a"* and the corresponding square of the absolute value of electric field is plotted in Fig. 1 (b) as dotted curve. The overlapping of the lossy Ge with the maximum electric field would allow strong absorption of the unwanted wavelength at λ = 454 nm. The calculated reflection spectrum is shown by the dotted curve in Fig. 2. As expected, the wavelengths around λ = 454 nm are nearly totally absorbed,

and the reflection spectrum turns to a flat-bottom shape. In comparison, if the Ge film is located at the node position (labeled as *"b"*) of the wavelength at λ = 454 nm, the wavelength around λ = 454 nm is still visible in the reflection spectrum as shown by the dashed curve in Fig. 2. The corresponding optical field is also plotted in Fig. 1 (b) as dashed curve. It is noted that the broadband absorption feature in our structure can be considered to originate from absorptions of two overlapped resonant modes. As evident from Fig. 2, due to their finite spectral linewidth, field intensities of the two cavity modes at λ = 370 nm and λ = 597 nm spread in wavelength, and overlap in the spectral band around λ = 454 nm, where the lossy Ge was placed at an antinode position. The broadband absorption around λ = 454 nm therefore can be considered as superimposed absorptions of the two resonant cavity modes at λ = 370 nm and λ = 597 nm.

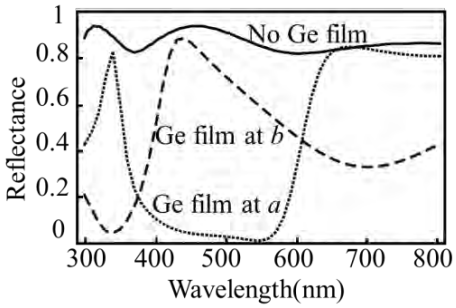

Fig. 2 Calculated reflection spectra of the cavity without absorbing Ge film, and with absorbing Ge film placed at position *"a"* and *"b"*, respectively.

3. Experimental Results and Discussion

To verify our theoretical design, we fabricated the proposed multi-layer structure. First, a thick Al film was deposited by standard electron beam evaporation onto a silicon wafer, and then a 182 nm-thick SU-8 photoresist was spin coated on top of the Al at a speed of 2500 r/min for 40 s. Next, a 13.6 nm-thick Ge film was deposited on top of the SU-8 photoresist film by electron beam evaporation. Lastly, another SU-8 photoresist layer with a thickness of 72 nm was spun on the top of the Ge layer to form the second dielectric layer. With these layered thicknesses, the Ge film is placed at the antinode position of the wavelength around λ = 454 nm. The thicknesses of the Ge and SU-8 photoresist films were obtained with variable angle spectroscopic ellipsometry measurements on separate silicon reference samples fabricated under the same conditions. Reflection spectrum of the sample was measured at a fixed angle of 7° from normal incidence. The measured reflection spectrum is shown as solid curve in Fig. 3. A nearly perfect rectangular broadband absorption (>90%) between 400 nm and 575 nm is measured, which is a good agreement with the calculated result shown in dotted curve, validating our mode-selective absorption design approach.

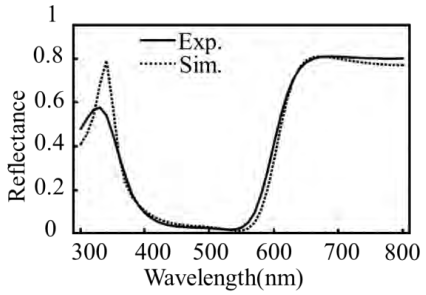

Fig. 3 Measured and Simulated reflection spectra of the sample.

Since the optical modes of a dielectric cavity depend on layer thickness, the reflection spectrum based upon our proposed mechanism of mode-selective absorption is tunable. As an example, Fig. 4 shows the calculated reflection spectra as we place a 14 nm Ge film at the antinodes of different wavelengths for different cavity sizes. For the three cavities with size of d = 250 nm, 270 nm, 290 nm, the 14 nm-thick Ge film is placed at antinode positions of 184 nm, 198 nm, 200 nm, respectively,

which corresponding the absorbing wavelength around λ = 427 nm, 457 nm, 488 nm. The reflection spectra show a consistent redshift of broadband absorption.

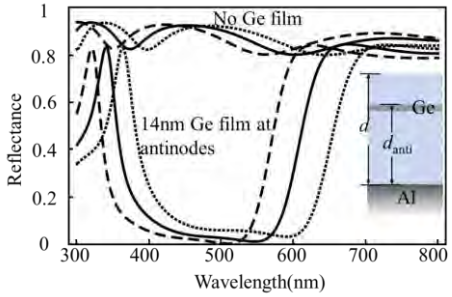

Fig. 4 Reflection spectra by placing a 14 nm Ge film at the antinodes of Different wavelengths for three different cavity sizes of *d*=250 nm (dash curve), 270 nm (solid curve) , 290 nm (dotted curve).

Furthermore, not only flat bottom of reflection spectrum, but also the narrow peak is desired in somewhere like physical colors with very high saturation. To obtain the narrow reflection peak, we also investigate the situation of placing the absorbers at the nodes of standing wave modes. The reflection spectra of ultra-thin carbon films placed on the top or inside of the dielectric layer are plotted in Fig. 5.

Here carbon is chosen as the absorber layer due to its capability of uniform absorption in the visible lights. In Fig. 5 (a), the dashed curve is the reflection spectrum of a 2 nm carbon film on a SU-8 layer with the thickness of 316 nm on the Al substrate. The reflection peak at the wavelength of 530 nm has a node at the top of SU-8 layer. To obtain the desired narrow peak at this wavelength, another carbon film with the thickness of 10 nm is inserted in the SU-8 layer at the node of this second order mode of standing wave, namely at the optimized location of 158nm from the Al substrate. Finally, this second order of standing wave mode remains while the third order mode at the wavelength of 360 nm is absorbed significantly which creates a dramatic drop in the reflection spectrum. Finally, only one reflection peak at the wavelength of 530 nm exists in the visible range. Notably, in this situation of placing two absorbers at the nodes of wanted wavelength, single reflection peak with the Full width at half maximum (FWHM) of 168 nm is achieved. Increase the layers of absorbers, narrower reflection peak is expected. In Fig. 5 (b), the dashed curve is the reflection spectrum of a 2 nm carbon film on a SU-8 layer of 380 nm on the Al substrate. Two carbon films with the thickness of 10 nm are inserted in the SU-8 layer at the nodes of this third order of standing wave mode at the wavelength of 430 nm, namely at the optimized locations of 127nm and 255nm from the Al substrate. Finally, this mode remains while the other modes at the wavelengths of 330 nm and 650 nm are absorbed effectively. The FWHM of reflection peak at the wavelength of 430 nm is only 85nm which creates a blue color with very high saturation. It indicates the possibility of scalable manufacturing of physical color via a sample layered structure.

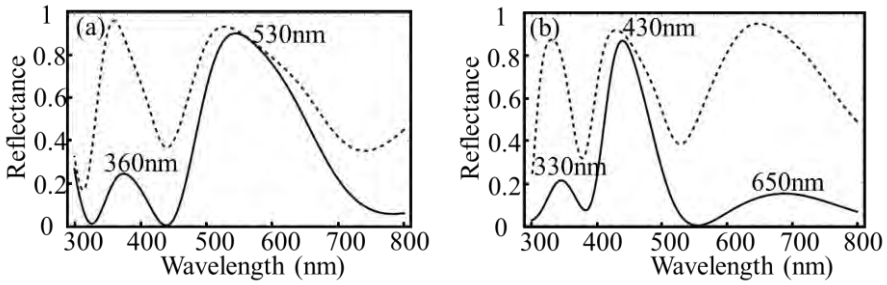

Fig. 5 Reflection spectra of carbon films at the nodes of different standing wave modes of dielectric cavity. Dashes: only carbon film on the top of the SU-8 cavity; solids: carbon films on top and inside of the SU-8 cavity. (a) 2nm carbon film on top layer and 10nm carbon film at the node of the second order mode of standing wave at the wavelength of 530nm with the cavity thickness of 316nm; (b) 2nm carbon film on top layer and two layers of 10nm carbon film at the nodes of the third order mode of standing wave at the wavelength of 430nm with the cavity thickness of 380nm;

4. Conclusions

In conclusion, we have demonstrated a mode-selective absorption mechanism in a planar thin-film structure. The spectral of a dielectric optical cavity were established to determine the positions of the embedded lossy layers for effective shaping the reflection spectrum. By placing lossy thin layer of Ge at the antinode of a target an unexpected wavelength of a dielectric cavity, a broadband spectrum of flat-bottom was demonstrated both in theory and experiment. Besides broadband absorption, multi-layer structure with ultra-thin carbon films to shape the spectrum into narrow reflection peaks are also discussed in theory. In the physics, the absorption mechanism of this method can be understood as all the ultra-thin lossy layers are located at each nodes of a standing wave mode with a certain wavelength. After infinitely passing through the lossy layers, the energy of undesired wavelengths will be totally absorbed. This manipulation of modes is tunable and shapes the spectrum arbitrarily within the thickness less than the wavelength. On the other hand, the simple layer structure without any patterns is suitable for scalable manufacturing. In the industries, the difficulty of red physical color can be solved by this method. It is also universally applicable for the entire electromagnetic wave spectrum. Since it is not very dependent on the properties of materials and the main control parameter of this method is the thickness of each layer, it can be widely considered as the broadband absorber or modes selector in the other frequency bands.

Acknowledgments

National Natural Science Foundation of China (NSFC) (61421002, 61575036, 61875030); Changjiang Scholar Program of Chinese Ministry of Education; National Science Foundation (NSF) of the United States (CMMI-1530547).

References

[1]. Wang, Y., X. Dong, and I.J. Fair, Spectrum shaping and NBI suppression in UWB communications. IEEE transactions on wireless communications, 2007. 6(5).

[2]. Wang, C. and J. Yao, Chirped microwave pulse generation based on optical spectral shaping and wavelength-to-time mapping using a Sagnac loop mirror incorporating a chirped fiber Bragg grating. Journal of Lightwave Technology, 2009. 27(16): p. 3336-3341.

[3]. Talley, C.E., et al., Surface-enhanced Raman scattering from individual Au nanoparticles and nanoparticle dimer substrates. Nano letters, 2005. 5(8): p. 1569-1574.

[4]. Kreibig, U. and M. Vollmer, Optical properties of metal clusters. Vol. 25. 2013: Springer Science & Business Media

[5]. Kreibig, U., E.R. Hummel, and P. Wissmann, Handbook of Optical Properties. Vol. II. Optics of Small Particles, Interfaces, and Surfaces. 1997, London: CRC Press.

[6]. Kristensen, A., et al., Plasmonic colour generation. Nature Reviews Materials, 2016. 2: p. 16088.

[7]. Kumar, K., et al., Printing colour at the optical diffraction limit. Nat Nanotechnol, 2012. 7(9): p. 557-61.

[8]. Li, Z., A.W. Clark, and J.M. Cooper, Dual Color Plasmonic Pixels Create a Polarization Controlled Nano Color Palette. ACS Nano, 2016. 10(1): p. 492-8.

[9]. Clausen, J.S., et al., Plasmonic metasurfaces for coloration of plastic consumer products. Nano Lett, 2014. 14(8): p. 4499-504.

[10]. Goh, X.M., et al., Three-dimensional plasmonic stereoscopic prints in full colour. Nat Commun, 2014. 5: p. 5361.

[11]. Xue, J., et al., Scalable, full-colour and controllable chromotropic plasmonic printing. Nat Commun, 2015. 6: p. 8906.

[12]. Moores, A. and F. Goettmann, The plasmon band in noble metal nanoparticles: an introduction to theory and applications. New Journal of Chemistry, 2006. 30(8): p. 1121-1132.

[13]. Liz-Marzán, L.M., Nanometals: formation and color. Materials today, 2004. 7(2): p. 26-31.

[14]. Munk, B.A., Frequency selective surfaces theory and design. john Wiley&Sons. 2000, Inc.

[15]. Xu, T., et al., Structural colors: from plasmonic to carbon nanostructures. Small, 2011. 7(22): p. 3128-3136.

[16]. Yue, W., et al., Color filters based on a nanoporous Al-AAO resonator featuring structure tolerant color saturation. Optics express, 2015. 23(21): p. 27474-27483.

[17]. Oller, D., et al., Scalable physical coloration. Materials Research Bulletin, 2016. 83: p. 556-562.

[18]. Kats, M.A., et al., Nanometre optical coatings based on strong interference effects in highly absorbing media. Nature materials, 2013. 12(1): p. 20-24.

[19]. Billmeyer, F.W., Color Science: Concepts and Methods, Quantitative Data and Formulae, by Gunter Wyszecki and WS Stiles, John Wiley and Sons, New York, 1982, 950 pp. Price: $75.00. 1983, Wiley Online Library.

[20]. M. A. Kats, R. Blanchard, P. Genevet, and F. Capasso, Nanometre optical coatings based on strong interference effects in highly absorbing media, Nat. Mater. 12, 24 (2012).

[21]. A. Borreman, S. Musa, A.A.M. Kok, M. B. J. Diemeer and A. Driessen, Fabrication of polymeric multimode waveguides and devices in SU-8 photoresist using selective polymerization, P. S. IEEE/LEOS Benelux Chapter, Amsterdam (2002).

[22]. A. Larsson, J. Maserjian, Optically addressed asymmetric Fabry-Perot modulator, Appl. Phys. Lett. 59, 3099 (1991).

[23]. G. Kang, I. Vartiainen, B. Bai, and J. Turunen, Enhanced dual-band infrared absorption in a Fabry-Perot cavity with subwavelength metallic grating, Opt. Express 19, 770(2011).